Deprotonation of group 14 metal amide complexes bearing ditopic carbanionic N-heterocyclic carbene ligands. Constitutional isomerism and dynamic behaviour.

*Jordan B. Waters, Lajoy S. Tucker and Jose M. Goicoechea**

Department of Chemistry, University of Oxford, Chemistry Research Laboratory, 12 Mansfield Road, Oxford, OX1 3TA, U.K.

E-mail: jose.goicoechea@chem.ox.ac.uk

Abstract

The reactivity of the lithiated N-heterocyclic carbene $[:C[N(2,6\text{-}^{i}Pr_2C_6H_3)]_2(CH)CLi]_\infty$ with two-coordinate homoleptic group 14 amides $E[N(SiMe_3)_2]_2$ (E = Sn, Pb) is described. Solutions of these mixtures readily result in the formal loss of one equivalent of bis(trimethylsilyl)amine, $HN(SiMe_3)_2$, to afford novel metallacycles. Reactions involving $Sn[N(SiMe_3)_2]_2$ initially give rise to the anionic complex $[\{:C[N(2,6\text{-}^{i}Pr_2C_6H_3)]_2C(CH)\}Sn\{N(SiMe_3)_2\}_2]^-$ (**1**), which eventually affords the novel distannane $[\{(THF)_2Li:C[N(2,6\text{-}^{i}Pr_2C_6H_3)]_2(CH)C\}Sn\{\mu\text{-}\kappa^1\text{:}\kappa^1\text{-}N(SiMe_3)(SiMe_2CH_2)\}Sn\{C(CH)[N(2,6\text{-}^{i}Pr_2C_6H_3)]_2C:\}\{N(SiMe_3)_2\}]$ (**2**) in which one of the trimethylsilyl substituents has been deprotonated and bridges the Sn–Sn bond affording a five-membered metallacycle. By contrast, reactions involving $Pb[N(SiMe_3)_2]_2$ give rise to a species that may be considered a constitutional isomer of **2**, $[\{(THF)_2Li:C[N(2,6\text{-}^{i}Pr_2C_6H_3)]_2(CH)C\}Pb\{N(SiMe_3)\}_2\{C(CH)[N(2,6\text{-}^{i}Pr_2C_6H_3)]_2C:\}Pb\{\kappa^2\text{-}N(SiMe_3)(SiMe_2CH_2)\}]$ (**3**), featuring a base-stabilised plumbylene species. The dynamic behaviour of **3** in solution suggests stereochemical inversion at the plumbylene moiety, $Pb\{\kappa^2\text{-}N(SiMe_3)(SiMe_2CH_2)\}$, a process which can be retarded at low temperatures allowing

for the observation of the two inequivalent proton environments of the methylene bridge. This process is believed to involve rapid intermolecular transfer of the plumbylene fragment between the ditopic carbanionic carbene ligands of the plumbyl core.

1. Introduction

Over the course of the last twenty five years, N-heterocyclic carbenes (NHCs) have developed into one of the most prominent families of supporting ligands in transition metal and main group chemistry.[1,2] Following Arduengo's seminal isolation of the first isolable N-heterocyclic carbene,[3] the chemistry of these compounds has developed at a dramatic pace and their use is now commonplace in fields ranging from organocatalysis to the isolation of highly reactive small molecules. Amongst the wide range of carbenes available, imidazol-2-ylidenes are arguably the most commonly used due to their ease of synthesis and highly tuneable steric properties. These species are now commonly employed in a variety of areas.

Despite their widespread use as supporting ligands, it has been demonstrated on a number of occasions that imidazol-2-ylidenes are not chemically inert and that they are susceptible to a variety of C–H, C–C and C–N bond activation processes. For example, the backbone protons of such species are relatively acidic and can be deprotonated in the presence of a strong base (such as ^{n}BuLi) as recently demonstrated by Robinson and co-workers.[4] The resulting compound is a ditopic carbanionic carbene, capable of binding to Lewis acids via both the backbone C4/C5 position and the carbenic C2 position. During the last five to six years the chemistry of such compounds has been extensively explored.[5] A number of studies detailing their isolation in the coordination sphere of alkali and alkaline-earth,[4,6] transition and post-transition metals,[7] and main group elements have been reported.[8] Recently their reactivity towards small molecules such as NO_2 has also been explored.[9]

We have a long-standing interest in the chemistry of ditopic carbanionic carbenes, specifically with regard to their use in the stabilisation of unusual main group element compounds. Herein we describe the reactivity of the lithiated N-heterocyclic carbene $[:C[N(2,6\text{-}^{i}Pr_2C_6H_3)]_2(CH)CLi]_\infty$ with two-coordinate homoleptic group 14 amides $E[N(SiMe_3)_2]_2$ (E = Sn, Pb), and show that solutions of such mixtures readily result in the deprotonation of one of the trimethylsilyl substituents to afford novel metallacycles. Despite their chemical similarities, the outcome of these reactions differs significantly for $Sn[N(SiMe_3)_2]_2$ and $Pb[N(SiMe_3)_2]_2$, and while both reactions give rise to species with comparable formulae (constitutional isomers) the bonding in such species varies dramatically. In the former case, the resulting compound is best described as a bridged distannane, whereas in the latter, the product of the reaction is a base-stabilised plumbylene.

2. Results and discussion

2.1. Reactivity of $[:C[N(2,6\text{-}^{i}Pr_2C_6H_3)]_2(CH)CLi]_\infty$ with $Sn[N(SiMe_3)_2]_2$

We have previously reported that addition of $[:C[N(2,6\text{-}^{i}Pr_2C_6H_3)]_2(CH)CK]_\infty$ to $Sn[N(SiMe_3)_2]_2$ in THF affords the anionic complex $[\{:C[N(2,6\text{-}^{i}Pr_2C_6H_3)]_2C(CH)\}Sn\{N(SiMe_3)_2\}_2]^-$ (**1**) which was structurally characterised as a [K(18-crown-6)]$^+$ salt in [K(18-crown-6)(THF)$_2$][**1**]·0.5THF.[6a] Interestingly, contrasting reactivity is observed for the lithium salt of same ditopic carbanionic N-heterocyclic carbene, $[:C[N(2,6\text{-}^{i}Pr_2C_6H_3)]_2(CH)CLi]_\infty$. Dissolution of a 1:1 mixture of $[:C[N(2,6\text{-}^{i}Pr_2C_6H_3)]_2(CH)CLi]_\infty$ and $Sn[N(SiMe_3)_2]_2$ in THF gives rise to the initial formation of **1** as evidenced by NMR spectroscopy, however upon slow diffusion of hexane into the reaction mixture, a novel distannane species, $[\{(THF)_2Li:C[N(2,6\text{-}^{i}Pr_2C_6H_3)]_2(CH)C\}Sn\{\mu\text{-}\kappa^1\text{:}\kappa^1\text{-}N(SiMe_3)(SiMe_2CH_2)\}Sn\{C(CH)[N(2,6\text{-}^{i}Pr_2C_6H_3)]_2C:\}\{N(SiMe_3)_2\}]$ (**2**), crystallised from the solution in good yields. In such a mixed polarity medium, it is reasoned that the amide

ligands are fairly labile allowing for the formation of aggregates of the type $\{Li[N(SiMe_3)_2]\}_x$ which are soluble in the THF/hexane mixture. The exact nature of such aggregates is undetermined and likely to be a complex equilibrium of different species whose concentration may vary as hexane diffuses into the solution.

Upon formal elimination of one equivalent of $Li[N(SiMe_3)_2]$ from **1**, we postulate that a stannylene intermediate forms, $Sn\{C(CH)[N(2,6\text{-}^{i}Pr_2C_6H_3)]_2C:\}\{N(SiMe_3)_2\}$ (**I1**, Scheme 1). This species would be susceptible to dimerisation to form a distannene (**I2)**. At this point, the $\{Li[N(SiMe_3)_2]\}_x$ by-product is suitably basic to deprotonate of one of the $SiMe_3$ groups of the distannene intermediate giving rise to bis(trimethylsilyl)amine. The resulting carbanion is believed to attack the Sn=Sn double bond thereby forming a five-membered heterocycle containing a single Sn–Sn bond.

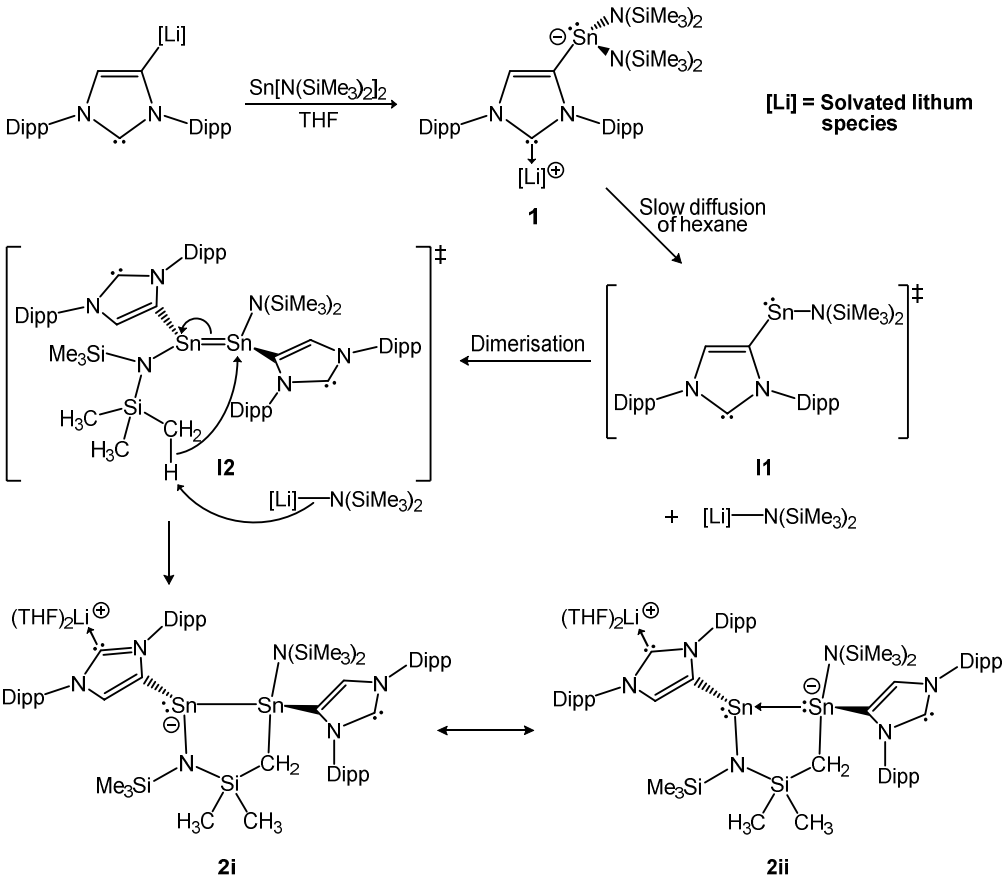

Scheme 1. Postulated mechanism for the formation of the distannane, **2**.

There are a handful of reported examples of the bis(trimethylsilyl)amide ligand being deprotonated in basic reaction media to afford metallacycles.[10–14] The basicity of the amide by-product is likely to also be increased due to the presence of IPr in solution. IPr has been shown to readily coordinate to lithium cations, hence, any amide aggregates which may form in solution are likely to be more basic, much as the reactivity of ^{n}BuLi is enhanced by the addition of a chelating ligand such as TMEDA (tetramethylethylenediamine).[15]

The distannane, **2**, was isolated in 54% crystalline yield and characterised by ^{1}H, ^{13}C{^{1}H}, ^{29}Si{^{1}H} and ^{119}Sn{^{1}H} NMR spectroscopy. The two distinct aIPr ligands can be easily identified by the diagnostic imidazole proton resonances which appear at 7.04 and 6.89 ppm in the ^{1}H NMR spectrum in d_8-THF. In line with a large degree of restricted rotation about the N–Dipp bonds, individual methine resonances which integrate to a single proton can be identified at 3.33, 3.19, 3.06, 2.95 and 2.89 ppm along with three more overlapping methine resonances between 2.87 and 2.78 ppm. Correspondingly, there are numerous overlapping doublet resonances attributable to the various methyl groups of the Dipp substituents between 0.93 and 1.46 ppm. The formation of the metallacycle can be clearly demonstrated by the inequivalence of the $SiMe_3$ groups.

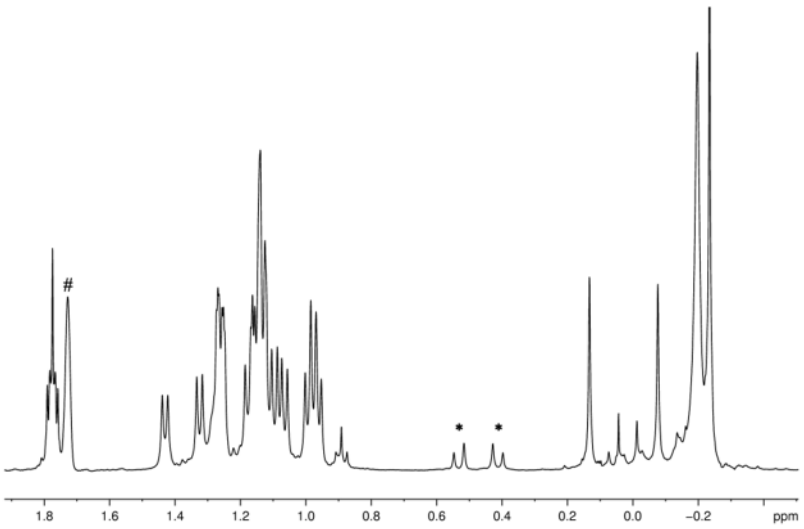

Figure 1. ^{1}H NMR spectrum of the aliphatic region of **2** in d_8-THF. Resonances marked with * are due to the CH_2 bridge of the metallacycle. The resonance marked with # is due to residual protons in the NMR solvent.

Most notably, the two inequivalent methyl groups bound to the silicon atom which forms part of the five-membered metallacycle appear as two separate resonances in the ^{1}H NMR spectrum at 0.13 and –0.08 ppm. Likewise, the two inequivalent protons of the tin bound carbon atom which forms part of the metallacycle appear as two doublets which couple to one another with a coupling constant of 12 Hz (Figure 1). The asymmetric metallacycle can also be observed by the presence of three resonances in the ^{29}Si{^{1}H} NMR spectrum in an approximate 2:1:1 ratio as expected. The ^{13}C{^{1}H} NMR spectrum gives rise to two highly downfield resonances at 221.9 and 215.7 ppm which can be assigned to the two carbenic positions. The resonance at 215.7 ppm is broadened with a *full width at half maximum* (fwhm) of approximately 20 Hz which likely results from coupling to the 92.4% abundant, quadrupolar, ^{7}Li nucleus (I = $^{3}/_{2}$). Lastly, the ^{119}Sn NMR spectrum clearly shows two resonances at –12.5 and –126.2 ppm due to the presence of two inequivalent tin environments (Figure 2).

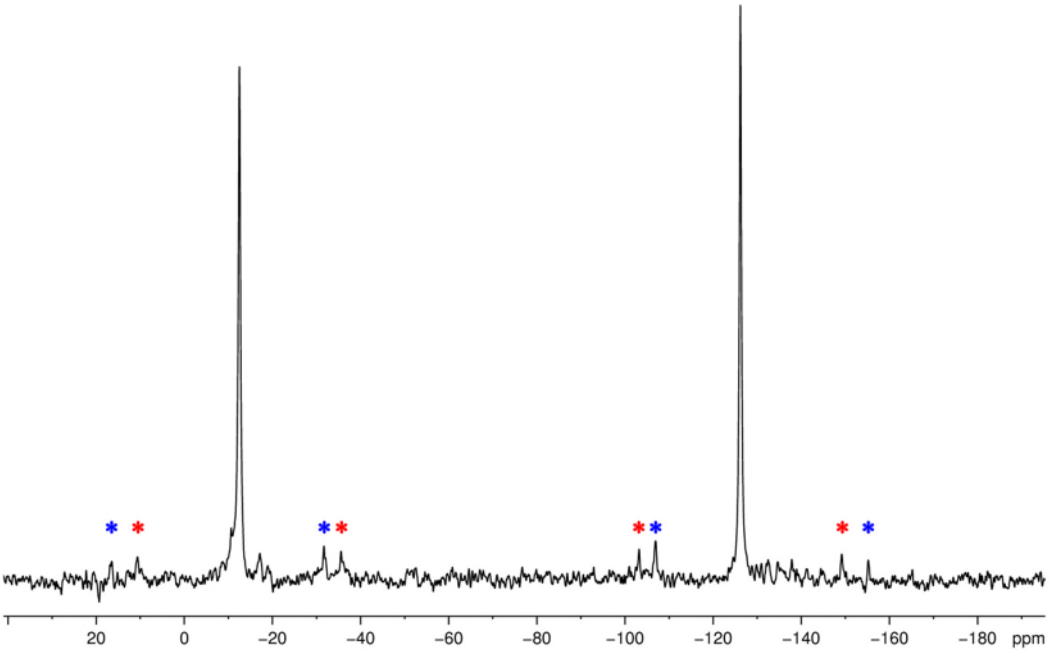

Figure 2. ^{119}Sn{^{1}H} NMR spectrum of **2** in d_8-THF. Resonances marked with * are satellites which result from ^{119}Sn coupling to ^{117}Sn. Resonances marked with * are satellites which result from ^{119}Sn coupling to ^{119}Sn.

The chemical shifts are indicative of shielded tin environments and neither are consistent with a stannylene (which typically give rise to notably downfield-shifted resonances), hence the resonance structure which shows a formal Sn–Sn bond (**2i**, Scheme 1) is a better description than that of a stannylene stabilised by lone pair donation from a trigonal pyramidal tin(II) anion (**2ii**, Scheme 1). The bonding between the two tin centres is further corroborated by the large coupling constant observed as satellites in the ^{119}Sn{^{1}H} NMR spectrum. The $^{1}J_{^{119}\mathrm{Sn}-^{117}\mathrm{Sn}}$ is measured to be approximately 8600 Hz and is symmetrically disposed about the central resonance as expected (Figure 2). The $^{1}J_{^{119}\mathrm{Sn}-^{119}\mathrm{Sn}}$ coupling constant was measured to be just under 9000 Hz. These satellites are not symmetric about the main resonance which can be accounted for due to second order effects. The ratio of the difference in chemical shift ($\Delta\delta$) and the coupling constant (J) is relatively small (i.e. $\Delta\delta/J \approx 2.4$). These second order effects result in the inner resonance of the respective doublet increasing in

intensity and the outer resonance decreasing; the main resonance lying at the intensity weighted mid-point of the satellite and not just equidistant from the two. The coupling constants are particularly large for a one-bond coupling interaction which may be indicative of a strong single bond between the two tin centres; coupling constants for hexaorganoditin compounds lie approximately in the range of 2000–4000 Hz.[16] The structure of **2** was unambiguously confirmed by single crystal X-ray diffraction which shows the formation of a strained Sn–C–Si–N–Sn metallacycle (Figure 3).

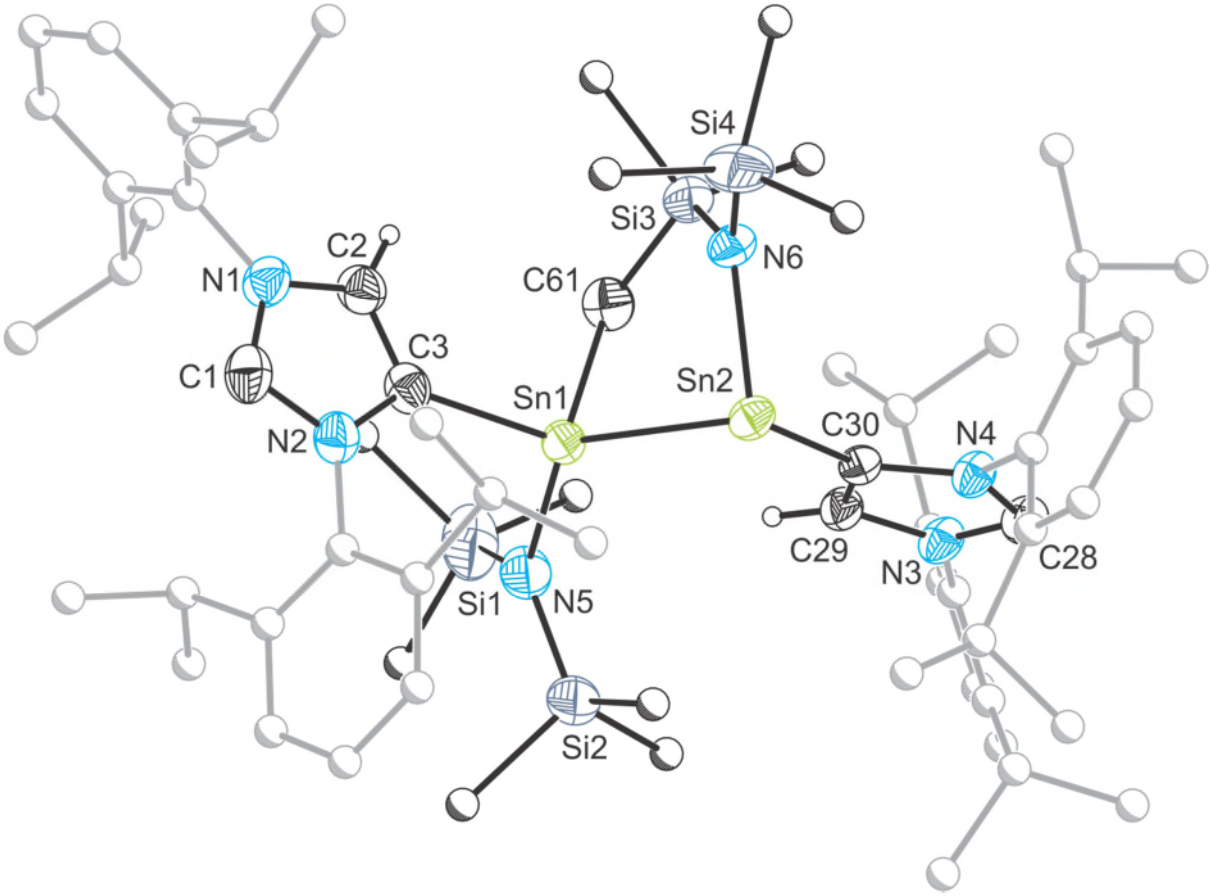

Figure 3. Molecular structure of **2**. Anisotropic displacement ellipsoids pictured are set at 50% probability. Hydrogen atoms (with the exception of the imidazole protons bonded to C2 and C29) and $[Li(THF)_2]^+$ have been omitted for clarity. Atoms of the Dipp groups and hydrogen atoms are pictured as spheres of arbitrary radii.

The five-membered metallacycle in **2** shows a significant amount of distortion as indicated by the very small angles about the tin atoms. Specifically, the Sn1–Sn2–N6 and Sn2–Sn1–C61 bond angles were found to be 83.7(1)° and 93.3(1)°, respectively. The geometry about Sn2 is trigonal pyramidal, $\Sigma_{\text{bond angles}}$ = 272.4°. Sn1 however, adopts a distorted tetrahedral geometry due to the inherent strain brought about by the five-membered ring. The four-coordinate geometry index, τ_4,[17] and the modified τ_4' parameter,[18] for Sn1 are 0.817 and 0.780, respectively, which indicate a fair degree of distortion from a perfect tetrahedral geometry (whereas, for example, the τ_4 and τ_4' values for Si3 are 0.958 and 0.955, respectively, indicating a near perfect tetrahedral geometry).

The Sn1–C3 and Sn2–C30 bond lengths, 2.186(4) and 2.256(3) Å, respectively, are within the expected range of bond lengths observed for abnormal bonding of an NHC to a tin centre.[6a,19] The aIPr coordinated to the lithium cation does show a significantly longer Sn–C bond length (Δd = 0.07 Å), however, this distance is very similar to that observed in other related complexes. The Sn1–C3 bond length is particularly short relative to other previously reported Sn–C bond distances. This is presumably due to the increased electrophilicity of Sn1 which is a four-coordinate tin centre (although still formally tin(II)) involved in a formal dative covalent bond with Sn2. The Sn–Sn bond length is measured to be 2.869(1) Å which is slightly longer than that expected based on the covalent radius of tin (r_{cov} = 1.39 Å; Σr_{cov} = 2.78 Å),[20,21] and is slightly longer than the distances observed in hexaphenylditin and a similar heterocyclic compound which resulted from loss of hydrogen from the trimethylsilylamide ligand, $[Sn\{N(SiMe_3)_2\}\{N(SiMe_3)(SiMe_2CH_2)\}]_2$,[12,22] for which Sn–Sn bond lengths are 2.770(4) and 2.737(2) Å, respectively. That being said, a search of the Cambridge Structural Database reveals a wide range in Sn–Sn bond lengths which easily extend beyond 3 Å indicating the elasticity of the bond whose length may be significantly

influenced by the steric influence of the ligands as much as the electronic properties of the bonding interaction.

2.2. Reactivity of [:C[N(2,6-^{i}Pr$_2$C$_6$H$_3$)]$_2$(CH)CLi]$_\infty$ with Pb[N(SiMe$_3$)$_2$]$_2$

When [:C[N(2,6-^{i}Pr$_2$C$_6$H$_3$)]$_2$(CH)CLi]$_\infty$ was added to a solution of Pb[N(SiMe$_3$)$_2$]$_2$ in d_8-THF, numerous products could be observed, but not accurately identified in the ^{1}H NMR spectrum of the crude reaction mixture. Slow diffusion of hexane into the THF reaction mixture allowed for the isolation of yellow crystals of a product that was identified by single crystal X-ray diffraction as [{(THF)$_2$Li:C[N(2,6-^{i}Pr$_2$C$_6$H$_3$)]$_2$(CH)C}Pb{N(SiMe$_3$)}$_2${C(CH)[N(2,6-^{i}Pr$_2$C$_6$H$_3$)]$_2$C:}Pb{κ^2-N(SiMe$_3$)(SiMe$_2$CH$_2$)}] (**3**) in approximately 20 % yield. This compound is formed by the deprotonation of an amide ligand much like that observed in the formation of **2**. In fact species **2** and **3** have identical molecular formula (with the exception of the group 14 elements) and can be considered constitutional isomers. In addition to the formation of **3**, extensive decomposition was also observed through the deposition of metallic lead. As the product has the core structure of the 2:1 adduct of [:C[N(2,6-^{i}Pr$_2$C$_6$H$_3$)]$_2$(CH)CLi]$_\infty$ and Pb[N(SiMe$_3$)$_2$]$_2$, which we have previously reported as the [K(18-crown-6)(THF)$_2$]$^+$ salt, [{:C[N(2,6-^{i}Pr$_2$C$_6$H$_3$)]$_2$C(CH)}$_2$Pb{N(SiMe$_3$)$_2$}]$^-$ (**4**),[6a] a higher yielding synthetic route was devised. Addition of Pb[N(SiMe$_3$)$_2$]$_2$ to a solution of **4** resulted in the quantitative formation of **3** over 24 hours with the generation of HN(SiMe$_3$)$_2$ as a by-product (Scheme 2).

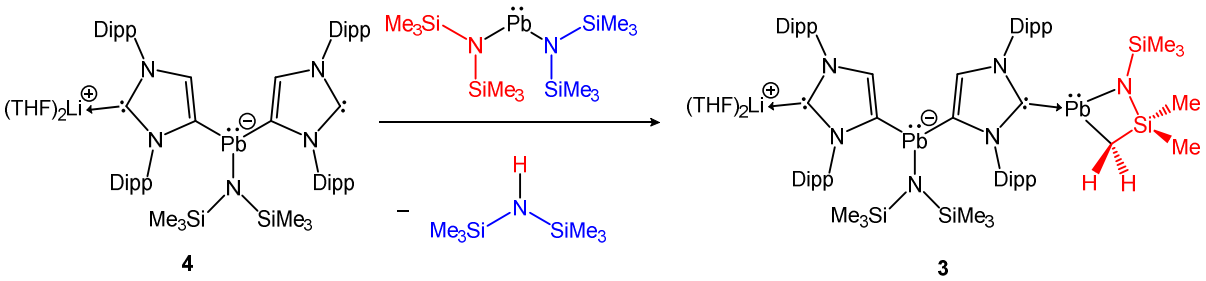

Scheme 2: Synthesis of **3** by the addition of $Pb[N(SiMe_3)_2]_2$ to $[\{:C[N(2,6\text{-}{}^{i}Pr_2C_6H_3)]_2C(CH)\}_2Pb\{N(SiMe_3)_2\}]^-$ (**4**).

It is likely that in a reaction of 1:1 stoichiometry numerous species form, potentially of the same form as those observed for **2**, i.e. species with a Pb–Pb bond incorporated into a metallacycle, however, if such a species were to form, it would be reasonable to assume that the strength of bonding between the two lead atoms would be quite weak and may be susceptible to decomposition under reaction conditions which generate $Li[N(SiMe_3)_2]$ and $HN(SiMe_3)_2$ as by-products. Computational studies reveal that the structure adopted by **3** is 29 $kJ{\cdot}mol^{-1}$ more stable that the hypothetical diplumbane isomer (i.e. the lead-containing analogue of **2**). Similarly, for **2**, the observed structure is also thermodynamically more stable than the constitutional isomer exhibiting the same geometry as **3** (albeit by only 11 $kJ{\cdot}mol^{-1}$). While these are purely net thermodynamic arguments and do not take into consideration possible formation pathways, they do help account for the rather distinct products observed for reactions that only differ in the nature of the group 14 element homoleptic amide reagents.

The ^1H NMR spectrum of **3** in d_8-THF reveals dynamic behaviour. Only a single resonance ascribed to protons on the imidazole ring was observed at 7.04 ppm (integrating to two protons). Similarly the methine and methyl group resonances observed are very similar to those previously reported for **4**. This implies that both carbanionic carbene ligands are identical in solution. Hence, the four-membered plumbylene metallacycle moiety must

equally reside on both carbene ligands or be dissociated in solution. The ^{1}H Diffusion-Ordered NMR spectrum (DOSY) of **3** reveals that all resonances attributable to **3**, i.e. both the plumbyl core and the plumbylene moiety diffuse at the same rate in solution, and therefore must be associated in solution on the timescale of the NMR experiment. The calculated *D* values were found to lie between 4.5×10^{-10} and 5.5×10^{-10} $m^2\cdot s^{-1}$ for all resonances, cf. 1.5×10^{-9} $m^2\cdot s^{-1}$ calculated for the $HN(SiMe_3)_2$ by-product. This shows that the plumbylene metallacycle is not a free species in solution as it would have a higher diffusion constant due to its smaller hydrodynamic radius relative to **4**. Therefore, it must be the case that the plumbylene metallacycle is free to change coordination from one of the NHC ligands to one of another species in solution, hence, both ligands appear identical by NMR spectroscopy.

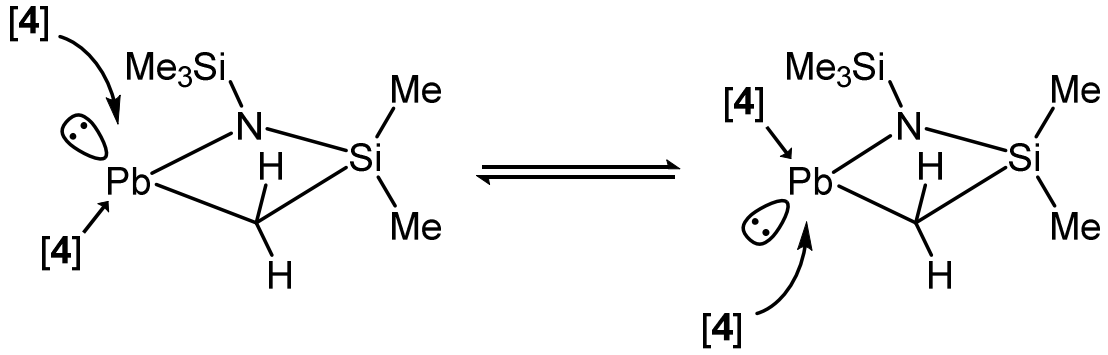

Figure 4: Illustration of the inversion of configuration that takes place in **3**.

Conclusive evidence for the formation of the four-membered Pb–N–Si–C metallacycle comes from the resonances which arise from the $SiMe_3$ groups. At room temperature, the ^{1}H NMR spectrum reveals four broad singlet resonances at –0.20, –0.41, –0.51 and –1.67 ppm in a ratio of 18:6:9:2 and these can be easily assigned to the $N(SiMe_3)_2$ group of the core, the two methyl groups of the metallacycle, the terminal N–$SiMe_3$ group, and the CH_2 group bonded to the lead atom forming the plumbylene. However, it would be expected that the methyl

groups and the CH_2 protons should give rise to separate resonances as part of a rigid metallacycle. It can be concluded that at room temperature, there is rapid inversion of configuration at the plumbylene lead atom resulting in the equivalence of these resonances (Figure 4). This presumably arises due to a concerted intermolecular exchange of the plumbyl moiety between carbenic centres, as opposed to via a formal dissociative process or a unimolecular pyramidal inversion. The computed bond dissociation energy for the interaction between one of the carbene sites of the plumbyl moiety and the plumbylene (C28–Pb2 as numbered in Figure 6) is 142 kJ·mol^{-1}. Likewise, the computed energy for the unimolecular pyramidal inversion is calculated to be greater than 95 kJ·mol^{-1}.

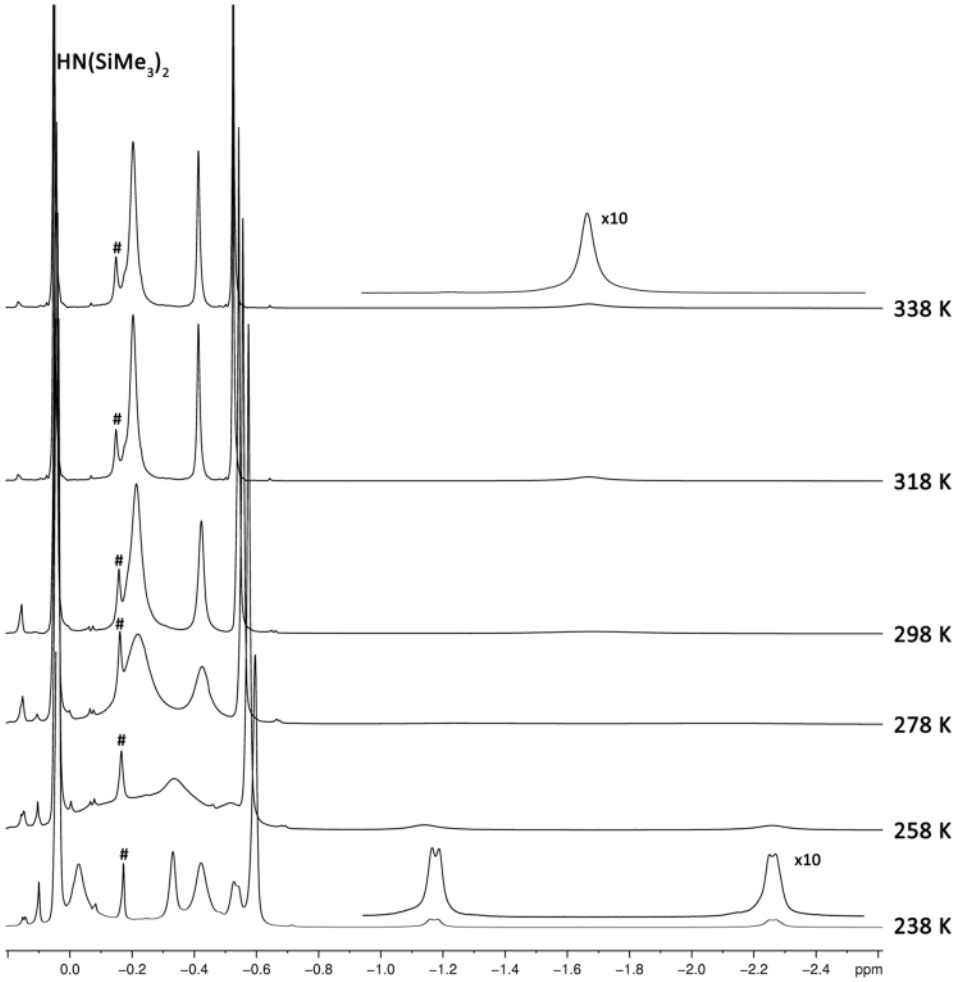

Figure 5. Variable temperature ^{1}H NMR of **3** in d_8-THF at 20 K intervals from 238 K to 338 K. Resonances marked with # arise from an unknown impurity.

This dynamic process could be observed by variable temperature ^{1}H NMR spectroscopy (Figure 5). On cooling the NMR sample from 298 K to 238 K, the single resonances observed for the CH_2 group and the two methyl groups broaden and separate into two resonances each due to the inequivalence of the two positions above and below the metallacycle. The two methyl groups give rise to resonances at –0.33 and –0.53 ppm which each integrate to three protons. Furthermore, the CH_2 protons give rise to doublet resonances due to mutual coupling at –1.17 and –2.26 ppm ($^{2}J_{H–H}$ = 11 Hz). The very upfield resonances are consistent with the environment of the CH_2 group which is bonded to a lead atom. These sets of resonances were observed to coalesce between 258 K and 278 K. Additionally upon heating the sample to 338 K, the broad resonances continued to reduce in line width as the rate of inversion increases. Analysis of these resonances allows for the calculation of the thermodynamic parameters for the dynamic process and reveals an enthalpy of activation ($\Delta H^{\ddagger}$) of 52(2) kJ·mol^{-1} and an entropy of activation ($\Delta S^{\ddagger}$) of –3(7) J·K^{-1}·mol^{-1} (see SI, Figure S13). With a Gibbs free energy of actiation ($\Delta G^{\ddagger}$) at 298 K of approximately 51 kJ·mol^{-1}, this confirms the dissociative process and the unimolecular inversion process are both too high in energy to take place under standard conditions and that a concerted intermolecular exchange is the most likely mechanism.

Finally, **3** was also characterised by $^{13}C\{^{1}H\}$, $^{29}Si\{^{1}H\}$ and $^{207}Pb\{^{1}H\}$ NMR spectroscopy. Two very broad resonances were observable in the $^{13}C\{^{1}H\}$ NMR spectrum at 200.0 and 193.9 ppm with a fwhm of approximately 500 and 100 Hz, respectively, due to the dynamic processes occurring at room temperature. These can be assigned to the C2 and C4 carbons of the imidazole ring. All carbon resonances for the silicon bound carbons can be observed and identified, except for the CH_2 carbon which is bonded to the lead atom of the plumbylene. It was however, possible to observe cross peaks for this resonance in a Heteronuclear Single

Quantum Coherence (HSQC) NMR experiment at 238 K. A cross peak was observed at 22.0 ppm in the ^{13}C domain which correlates with both doublet resonances observed for the inequivalent protons of the CH_2 bridge. As was the case in **2**, three resonances can be observed in the $^{29}Si\{^1H\}$ NMR spectrum of **3** as expected. Finally, the room temperature $^{207}Pb\{^1H\}$ NMR spectrum displays two extremely broad resonances at 2840.6 and 1674.6 ppm which can be assigned to the plumbylene lead atom and the central plumbyl lead atom, respectively (cf. 1619.2 ppm in $Li(THF)_2$·**4**).

The structure of **3** was unambiguously confirmed by single crystal X-ray diffraction. Single crystals were grown by slow diffusion of hexane into a THF solution. **3** was also fortuitously crystallised with the plumbylene moiety in both configurations providing crystallographic evidence for the inversion of configuration which is suggested to take place (Figures 6 and 7). Both isomers were found to crystallise in a Sohncke space group, that is one without a mirror plane or inversion symmetry, specifically $P2_1$. Both samples were determined to be enantiopure crystals with Flack parameters calculated at 0.070(5) and 0.025(4).[23]

The structural parameters for both isomers of **3** were found to be very similar, if not identical within experimental error. The Pb1–C3 bond lengths were observed to be 2.356(9) and 2.366(8) Å and the Pb1–C30 bond lengths 2.394(9) and 2.403(9) Å. The Pb1–C30 bond lengths are notably longer than those of the previously recorded Pb–C bond lengths by up to 0.5 Å, which may indicate a weaker bonding interaction as a result of the presence of the coordinating plumbylene metallacycle.

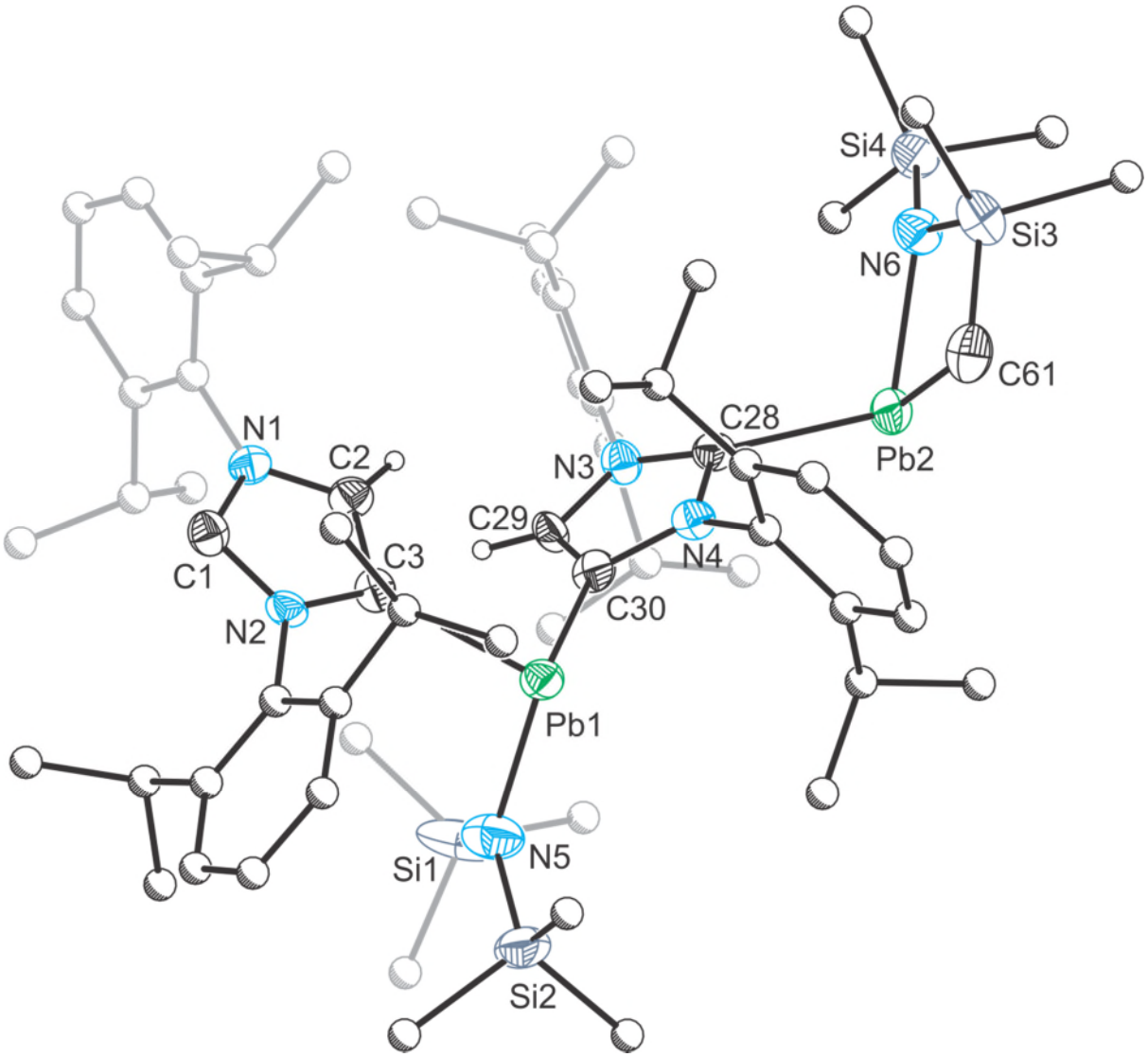

Figure 6. Molecular structure of *R*-**3**. Anisotropic displacement ellipsoids pictured are set at 50% probability. Hydrogen atoms (with the exception of the imidazole protons bonded to C2 and C29) and $[Li(THF)_2]^+$ have been omitted for clarity. Atoms of the Dipp groups and hydrogen atoms are pictured as spheres of arbitrary radii.

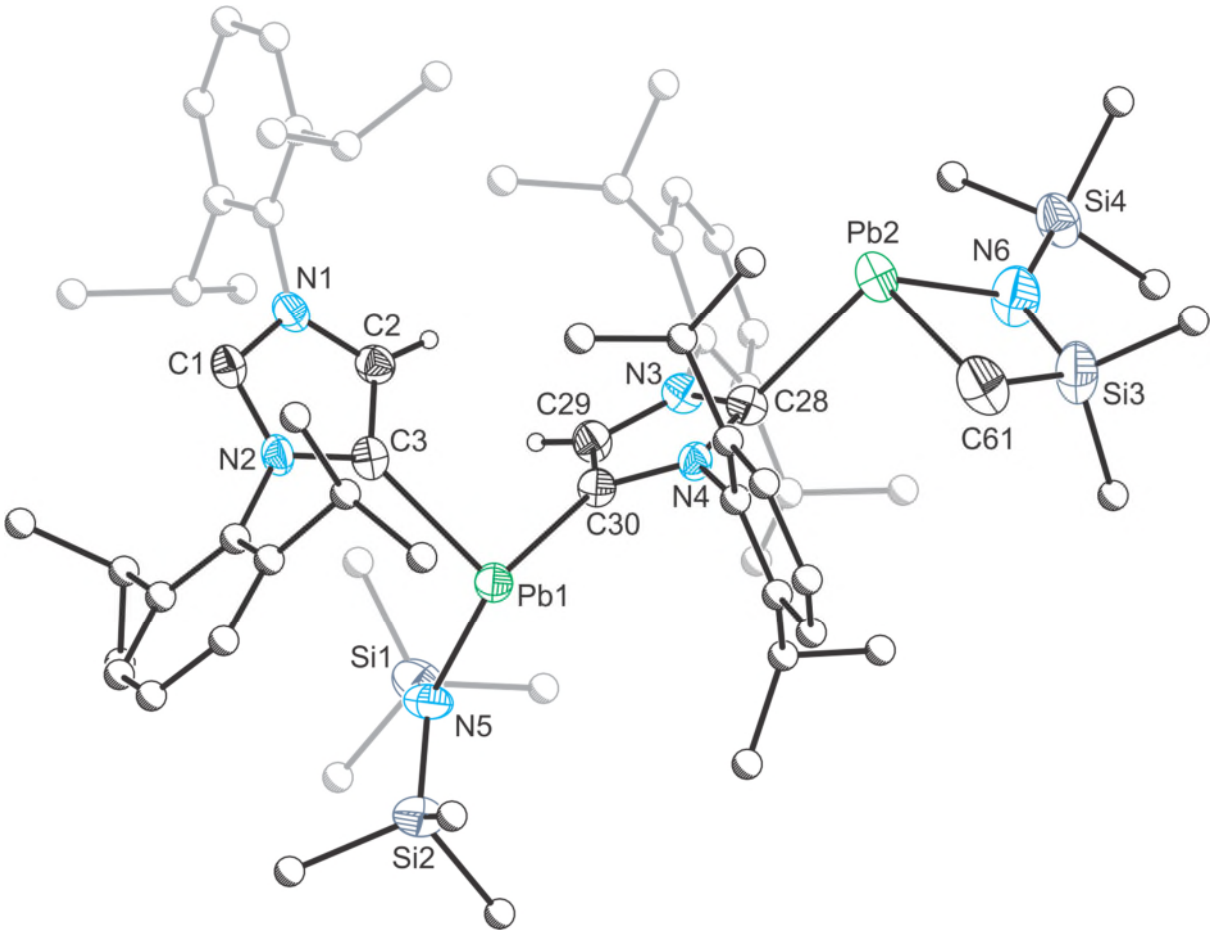

Figure 7. Molecular structure of *S*-**3**. Anisotropic displacement ellipsoids pictured are set at 50% probability. Hydrogen atoms (with the exception of the imidazole protons bonded to C2 and C29) and $[Li(THF)_2]^+$ have been omitted for clarity. Atoms of the Dipp groups and hydrogen atoms are pictured as spheres of arbitrary radii.

The Pb2–C28 bond distance was found to vary between the two isomers, however, both were still significantly longer than the other Pb–C distances observed in other related complexes at 2.472(9) and 2.522(9) Å. The large difference between the two isomers may just be a result of crystal packing. The bond lengths of Pb2 to both N6 and C61 were found to be shorter than other Pb–N and Pb–C bond lengths observed elsewhere. The Pb2–C61 distances, for example, are 2.325(13) and 2.327(11) Å and likely result due to the inherent strain of the four-membered metallacycle which preferentially brings the substituents closer so as to

increase the N6–Pb2–C61 bond angle which can be measured to be highly acute, 72.7(4)° and 73.2(4)°. In these two low energy conformations, the lead atom of the plumbylene unit retains a trigonal pyramidal geometry ($\Sigma_{\text{bond angles}}$ = 280.0° and 280.2°). Finally, the plumbylene unit does not coordinate directly in the plane with the carbene carbon of the NHC. This can be seen by the slight distortion from trigonal planar as would be expected for the carbene carbon ($\Sigma_{\text{bond angles}}$ = 351.5° and 351.7°). This is likely due to the steric bulk of the Dipp groups which forces the plumbylene metallacycle to coordinate slightly out of the plane of the imidazole ring.

3. Conclusions

We have shown that solutions of the lithiated N-heterocyclic carbene [:C[N(2,6-^{i}Pr$_2$C$_6$H$_3$)]$_2$(CH)CLi]$_\infty$ with two-coordinate group 14 amides E[N(SiMe$_3$)$_2$]$_2$ (E = Sn, Pb) result in the formal loss of bis(trimethylsilyl)amine to afford two novel metallacycles that can be thought of as constitutional isomers of one another. The tin-containing species can be rationalised as a distannane in which a deprotonated bis(trimethylsilyl)amide bridges the two tin centres. By contrast, reactions involving Pb[N(SiMe$_3$)$_2$]$_2$ afford a plumbyl-stabilised plumbylene species with interesting dynamic behaviour in solution. These results show that in basic media bis(trimethylsilyl)amide substituents can be readily deprotonated giving rise to complex mixtures involving a variety of species in solution. These findings notably contrast with previous observations involving the analogous potassium salt of the deprotonated 1,3-bis(2,6-diisopropylphenyl)-imidazol-2-ylidene ligand where such deprotonation reactions were not observed.[6a]

4. Experimental

General synthetic methods. All reactions and product manipulations were carried out under an inert atmosphere of argon or dinitrogen using standard Schlenk-line or glovebox techniques (MBraun UNIlab glovebox maintained at < 0.1 ppm H_2O and < 0.1 ppm O_2). $E[N(SiMe_3)_2]_2$ (E = Sn, Pb) and $[:C[N(2,6\text{-}^iPr_2C_6H_3)]_2(CH)CLi]_\infty$ were prepared according to previously reported literature procedures.[4,24,25] Hexane (hex; HPLC grade, >97%, Sigma-Aldrich) was purified using an MBraun SPS-800 solvent system. Tetrahydrofuran (THF; HPLC grade, ≥99.9%, Sigma-Aldrich) was distilled over a sodium metal/benzophenone mixture. d_8-THF (99.5%, Fluorochem) was dried over CaH_2, vacuum distilled and degassed before use. All dry solvents were stored under argon in gas-tight ampoules over activated 3 Å molecular sieves.

Analytical techniques. Single crystal X-ray diffraction data were collected using an Enraf-Nonius kappa-CCD diffractometer equipped with a 95 mm CCD area detector. Crystals were selected under Paratone-N oil, mounted on micromount loops and quench-cooled using an Oxford Cryosystems open flow N_2 cooling device.[26] Data were collected at 150 K using graphite monochromated Mo K_α radiation (λ = 0.71073 Å). Equivalent reflections were merged and the diffraction patterns processed with the DENZO and SCALEPACK programs.[27] Structures were subsequently solved using direct methods or using the charge flipping algorithm as implemented in the program SUPERFLIP,[28] and refined on F^2 using the SHELXL package.[29]

NMR samples were prepared inside an inert atmosphere glovebox in NMR tubes equipped with a gas-tight valve. ^1H and ^{13}C NMR spectra were acquired at 500.30 and 125.80 MHz, respectively on a Bruker AVII or AVIII NMR spectrometer. ^1H and ^{13}C spectra are reported

relative to TMS and were referenced to the most downfield residual solvent resonance (d_8-THF: δ_H 3.58 ppm, δ_C 67.6 ppm).

Elemental analyses were performed by Elemental Microanalysis Ltd., Devon. 10–15 mg samples were sent in sealed, evacuated Pyrex ampoules. All values are an average of at least two data collections and are given as percentages.

*Synthesis of [{(THF)$_2$Li:C[N(2,6-^{i}Pr$_2$C$_6$H$_3$)]$_2$(CH)C}Sn{μ-κ^1:κ^1-N(SiMe$_3$)(SiMe$_2$CH$_2$)}Sn{C(CH)[N(2,6-^{i}Pr$_2$C$_6$H$_3$)]$_2$C:}{N(SiMe$_3$)$_2$}] (**2**).* To a solution of [:C[N(2,6-^{i}Pr$_2$C$_6$H$_3$)]$_2$(CH)CLi]$_\infty$ (240 mg, 0.609 mmol) in THF (5 mL) was added a solution of Sn[N(SiMe$_3$)$_2$]$_2$ (268 mg, 0.609 mmol) in THF (5 mL) an the mixture stirred at ambient temperature. The orange solution was allowed to stir for 30 minutes before being filtered into a large crystallisation ampoule. Diffusion of hexane into a solution of the product and storage at 4 °C afforded yellow crystals after four days. The solution was periodically agitated for approximately two weeks to encourage mixing of the two solutions and crystallisation of the product until both solutions had fully mixed and no further crystallisation was observed. The yellow solution was decanted from the crystals which were then dried well under a dynamic vacuum (245 mg, 54% crystalline yield). Anal. Calcd for $C_{74}H_{121}LiN_6O_2Si_4Sn_2$ (1484.50): C 59.87%, H 8.28%, N 5.66%. Found: C 59.65%, H 8.00%, N 5.56%. ^{1}H NMR (500.30 MHz, d_8-THF): δ (ppm) 7.11–7.27 (m, 12H; *meta*-Dipp and *para*-Dipp); 7.04 (s, 1H; NCC*H*N); 6.89 (s, 1H; NCC*H*N); 3.62 (m, 8H; THF); 3.33 (sept, $^3J_{H–H}$ = 7 Hz, 1H; C$_6$H$_3${C*H*(CH$_3$)$_2$}$_2$); 3.19 (sept, $^3J_{H–H}$ = 7 Hz, 1H; C$_6$H$_3${C*H*(CH$_3$)$_2$}$_2$); 3.06 (sept, $^3J_{H–H}$ = 7 Hz, 1H; C$_6$H$_3${C*H*(CH$_3$)$_2$}$_2$); 2.95 (sept, $^3J_{H–H}$ = 7 Hz, 1H; C$_6$H$_3${C*H*(CH$_3$)$_2$}$_2$); 2.89 (sept, $^3J_{H–H}$ = 7 Hz, 1H; C$_6$H$_3${C*H*(CH$_3$)$_2$}$_2$); 2.78–2.87 (m, 3H; C$_6$H$_3${C*H*(CH$_3$)$_2$}$_2$); 1.77 (m, 8H; THF); 1.43 (d, $^3J_{H–H}$ = 7 Hz, 3H; C$_6$H$_3${CH(C*H*$_3$)$_2$}$_2$); 1.33 (d, $^3J_{H–H}$ = 7 Hz, 3H; C$_6$H$_3${CH(C*H*$_3$)$_2$}$_2$); 1.27

(d, $^{3}J_{H–H}$ = 7 Hz, 3H; $C_6H_3\{CH(CH_3)_2\}_2$); 1.26 (d, $^{3}J_{H–H}$ = 7 Hz, 3H; $C_6H_3\{CH(CH_3)_2\}_2$); 1.25 (d, $^{3}J_{H–H}$ = 7 Hz, 3H; $C_6H_3\{CH(CH_3)_2\}_2$); 1.18 (d, $^{3}J_{H–H}$ = 7 Hz, 3H; $C_6H_3\{CH(CH_3)_2\}_2$); 1.16 (d, $^{3}J_{H–H}$ = 7 Hz, 3H; $C_6H_3\{CH(CH_3)_2\}_2$); 1.12–1.16 (m, 12H; $C_6H_3\{CH(CH_3)_2\}_2$); 1.10 (d, $^{3}J_{H–H}$ = 7 Hz, 3H; $C_6H_3\{CH(CH_3)_2\}_2$); 1.06 (d, $^{3}J_{H–H}$ = 7 Hz, 3H; $C_6H_3\{CH(CH_3)_2\}_2$); 0.99 (d, $^{3}J_{H–H}$ = 7 Hz, 3H; $C_6H_3\{CH(CH_3)_2\}_2$); 0.98 (d, $^{3}J_{H–H}$ = 7 Hz, 3H; $C_6H_3\{CH(CH_3)_2\}_2$); 0.96 (d, $^{3}J_{H–H}$ = 7 Hz, 3H; $C_6H_3\{CH(CH_3)_2\}_2$); 0.53 (d, $^{2}J_{H–H}$ = 12 Hz, 1H; $N(Si(CH_3)_3)(Si(CH_3)_2CH_2)$); 0.41 (d, $^{2}J_{H–H}$ = 12 Hz, 1H; $N(Si(CH_3)_3)(Si(CH_3)_2CH_2)$); 0.13 (s, 3H; $N(Si(CH_3)_3)(Si(CH_3)_2CH_2)$); –0.08 (s, 3H; $N(Si(CH_3)_3)(Si(CH_3)_2CH_2)$); –0.20 (s, 18H; $N(Si(CH_3)_3)_2$); –0.23 (s, 9H; $N(Si(CH_3)_3)(Si(CH_3)_2CH_2)$). $^{13}C\{^{1}H\}$ NMR (125.80 MHz, d_8-THF): δ (ppm) 221.9 (CN_2); 215.7 (br, fwhm = 20 Hz; $LiCN_2$); 151.7 (NCCHN); 147.7, 147.5, 147.4, 147.3, 147.2, 147.0, 146.8, 146.2 (*ortho*-Dipp); 143.4 (*ipso*-Dipp); 143.0 (NCCHN); 142.8, 141.0, 140.6 (*ipso*-Dipp); 132.1, 130.9 (NCCHN); 128.4, 128.1 (×2), 128.0 (*para*-Dipp); 124.6, 123.9, 123.8, 123.7 (×2), 123.4, 123.3, 123.2 (*meta*-Dipp); 68.4 (THF); 29.9, 29.8, 29.1, 29.0, 28.9, 28.8, 28.7 (×2) ($C_6H_3\{CH(CH_3)_2\}_2$); 27.8, 26.9, 26.8 ($C_6H_3\{CH(CH_3)_2\}_2$); 26.6 (THF); 26.3, 26.2, 26.0, 25.9, 25.4, 25.0, 24.9, 24.8, 24.2, 24.1, 23.7, 22.9, 22.7 ($C_6H_3\{CH(CH_3)\}_2$); 15.2 ($Si(CH_3)_2CH_2$); 7.9, 7.4 ($Si(CH_3)_2CH_2$); 7.2 ($N(Si(CH_3)_3)(Si(CH_3)_2CH_2)$); 6.9 ($N(Si(CH_3)_3)_2$). $^{29}Si\{^{1}H\}$ NMR (99.32 MHz, d_8-THF): δ (ppm) –0.2 (s, $N(Si(CH_3)_3)(Si(CH_3)_2CH_2)$); –1.2 (s, $N(Si(CH_3)_3)(Si(CH_3)_2CH_2)$); –5.0 (s, $N(Si(CH_3)_3)_2$). $^{119}Sn\{^{1}H\}$ NMR (186.43 MHz, d_8-THF): δ (ppm) –12.5 (s; satellites $^{1}J_{^{119}Sn–^{117}Sn}$ = 8613 Hz, $^{1}J_{^{119}Sn–^{119}Sn}$ = 8977 Hz); –126.2 (s; satellites $^{1}J_{^{119}Sn–^{117}Sn}$ = 8570 Hz, $^{1}J_{^{119}Sn–^{119}Sn}$ = 8996 Hz).

Synthesis of $[\{(THF)_2Li:C[N(2,6\text{-}{}^{i}Pr_2C_6H_3)]_2(CH)C\}Pb\{N(SiMe_3)\}_2\{C(CH)[N(2,6\text{-}{}^{i}Pr_2C_6H_3)]_2C:\}Pb\{\kappa^{2}\text{-}N(SiMe_3)(SiMe_2CH_2)\}]$ ***(3)***. To a solution of $[Li(THF)_2][Pb\{C(CH)[N(2,6\text{-}{}^{i}Pr_2C_6H_3)]_2C:\}_2\{N(SiMe_3)_2\}]$ (247 mg, 0.191 mmol) in THF

(5 mL) was added a solution of $Pb[N(SiMe_3)_2]_2$ (101 mg, 0.191 mmol) in THF (5 mL) with stirring at ambient temperature. The yellow solution was allowed to stir overnight before being filtered. Diffusion of hexane into the filtrate afforded yellow crystals suitable for single crystal X-ray diffraction (220 mg, 69% crystalline yield). Anal. Calcd for $C_{74}H_{121}LiN_6O_2Pb_2Si_4$ (1660.51): C 53.53%, H 7.35%, N 5.06%. Found: C 51.46%, H 7.38%, N 5.37%. ^{1}H NMR (500.30 MHz, d_8-THF, 298 K): δ (ppm) 7.22–7.30 (m, 4H; *para*-Dipp); 7.12–7.20 (m, 8H; *meta*-Dipp); 7.04 (s, 2H; NCC*H*N); 3.62 (m, 8H; THF); 2.84–2.93 (m, 4H; $C_6H_3\{CH(CH_3)_2\}_2$); 2.81 (sept, $^3J_{H–H}$ = 7 Hz, 2H; $C_6H_3\{CH(CH_3)_2\}_2$); 2.76 (sept, $^3J_{H–H}$ = 7 Hz, 2H; $C_6H_3\{CH(CH_3)_2\}_2$); 1.77 (m, 8H; THF); 1.28 (d, $^3J_{H–H}$ = 7 Hz, 6H; $C_6H_3\{CH(CH_3)_2\}_2$); 1.18–1.23 (m, 12H; $C_6H_3\{CH(CH_3)_2\}_2$); 1.10–1.16 (m, 18H; $C_6H_3\{CH(CH_3)_2\}_2$); 1.07 (d, $^3J_{H–H}$ = 7 Hz, 6H; $C_6H_3\{CH(CH_3)_2\}_2$); 0.86 (br s, 6H; $C_6H_3\{CH(CH_3)_2\}_2$); –0.21 (br s, 18H; $N(Si(CH_3)_3)_2$); –0.42 (br s, 6H; $N(Si(CH_3)_3)(Si(CH_3)_2CH_2)$); –0.54 (s, 9H; $N(Si(CH_3)_3)(Si(CH_3)_2CH_2)$); –1.67 (v br s, 2H; $N(Si(CH_3)_3)(Si(CH_3)_2CH_2)$). ^{1}H NMR (500.30 MHz, d_8-THF, 338 K): δ (ppm) 7.23–7.30 (m, 4H; *para*-Dipp); 7.14–7.21 (m, 8H; *meta*-Dipp); 7.07 (s, 2H; NCC*H*N); 3.62 (m, 8H; THF); 2.92 (sept, $^3J_{H–H}$ = 7 Hz, 2H; $C_6H_3\{CH(CH_3)_2\}_2$); 2.88 (sept, $^3J_{H–H}$ = 7 Hz, 2H; $C_6H_3\{CH(CH_3)_2\}_2$); 2.83 (sept, $^3J_{H–H}$ = 7 Hz, 2H; $C_6H_3\{CH(CH_3)_2\}_2$); 2.77 (sept, $^3J_{H–H}$ = 7 Hz, 2H; $C_6H_3\{CH(CH_3)_2\}_2$); 1.77 (m, 8H; THF); 1.30 (d, $^3J_{H–H}$ = 7 Hz, 6H; $C_6H_3\{CH(CH_3)_2\}_2$); 1.17–1.23 (m, 12H; $C_6H_3\{CH(CH_3)_2\}_2$); 1.16 (d, $^3J_{H–H}$ = 7 Hz, 12H; $C_6H_3\{CH(CH_3)_2\}_2$); 1.13 (d, $^3J_{H–H}$ = 7 Hz, 6H; $C_6H_3\{CH(CH_3)_2\}_2$); 1.08 (d, $^3J_{H–H}$ = 7 Hz, 6H; $C_6H_3\{CH(CH_3)_2\}_2$); 0.87 (d, $^3J_{H–H}$ = 7 Hz, 6H; $C_6H_3\{CH(CH_3)_2\}_2$); –0.20 (br s, 18H; $N(Si(CH_3)_3)_2$); –0.41 (br s, 6H; $N(Si(CH_3)_3)(Si(CH_3)_2CH_2)$); –0.51 (s, 9H; $N(Si(CH_3)_3)(Si(CH_3)_2CH_2)$); –1.67 (br s, 2H; $N(Si(CH_3)_3)(Si(CH_3)_2CH_2)$). ^{1}H NMR (500.30 MHz, d_8-THF, 238 K): δ (ppm) 7.23–7.30 (m, 4H; *para*-Dipp); 7.10–7.34 (br m, 12H; *meta*-Dipp and *para*-Dipp); 7.06 (br s, 1H; NCC*H*N); 6.92 (v br s, 1H; NCC*H*N); 3.62

(m, 8H; THF); 2.56–3.00 (br m, 8H; $C_6H_3\{CH(CH_3)_2\}_2$); 1.77 (m, 8H; THF); 0.97–1.35 (br m, 48H; $C_6H_3\{CH(CH_3)_2\}_2$); –0.03 (br s, 9H; $N(Si(CH_3)_3)_2$); –0.33 (br s, 3H; $N(Si(CH_3)_3)(Si(CH_3)_2CH_2)$); –0.42 (br s, 9H; $N(Si(CH_3)_3)_2$); –0.53 (br s, 3H; $N(Si(CH_3)_3)(Si(CH_3)_2CH_2)$); –0.60 (s, 9H; $N(Si(CH_3)_3)(Si(CH_3)_2CH_2)$); –1.17 (d, $^2J_{H–H}$ = 11 Hz, 1H; $N(Si(CH_3)_3)(Si(CH_3)_2CH_2)$); –2.26 (d, $^2J_{H–H}$ = 11 Hz, 1H; $N(Si(CH_3)_3)(Si(CH_3)_2CH_2)$). $^{13}C\{^1H\}$ NMR (125.80 MHz, d_8-THF, 298 K): δ (ppm) 200.0 (v br, fwhm = 532 Hz; CN_2); 193.9 (br, fwhm = 104 Hz; NCCHN); 147.5, 147.3, 146.9, 146.4 (*ortho*-Dipp); 141.6 (br, fwhm = 31 Hz; *ipso*-Dipp); 139.0 (br, fwhm = 45 Hz; *ipso*-Dipp); 135.7 (br, fwhm = 16 Hz; NCCHN); 129.4 (br, fwhm = 9 Hz; *para*-Dipp); 128.9 (br, fwhm = 9 Hz; *para*-Dipp); 124.5, 124.3, 124.1, 123.8 (*meta*-Dipp); 68.4 (THF); 29.2, 29.1, 29.0, 28.9 ($C_6H_3\{CH(CH_3)_2\}_2$); 26.5 (THF); multiple overlapping broad and sharp resonances obscured by solvent resonance ($C_6H_3\{CH(CH_3)\}_2$); 14.6 (v br, fwhm = 99 Hz; $N(Si(CH_3)_3)(Si(CH_3)_2CH_2)$); 7.4 (br, fwhm = 9 Hz; $N(Si(CH_3)_3)_2$); 5.3 ($N(Si(CH_3)_3)(Si(CH_3)_2CH_2)$). The resonance corresponding to the ($N(Si(CH_3)_3)(Si(CH_3)_2CH_2)$) carbon environment cannot be observed. $^{29}Si\{^1H\}$ NMR (99.32 MHz, d_8-THF, 298 K): δ (ppm) –4.9 (s, $N(Si(CH_3)_3)(Si(CH_3)_2CH_2)$); –6.6 (s, $N(Si(CH_3)_3)_2$); –15.6 (s, $N(Si(CH_3)_3)(Si(CH_3)_2CH_2)$). $^{207}Pb\{^1H\}$ NMR (104.59 MHz, d_8-THF, 298 K): δ (ppm) 2840.6 (v br, fwhm = 4569 Hz; $(aIPr{\cdot}Li(THF)_2)Pb\{N(SiMe_3)_2\}$-$(aIPr{\cdot}Pb\{N(SiMe_3)SiMe_2CH_2\})$); 1674.6 (v br, fwhm = 2576 Hz; $(aIPr{\cdot}Li(THF)_2)Pb\{N(SiMe_3)_2\}(aIPr{\cdot}Pb\{N(SiMe_3)SiMe_2CH_2\})$).

Synthesis of $[\{(THF)_2Li:C[N(2,6\text{-}^iPr_2C_6H_3)]_2(CH)C\}:C[N(2,6\text{-}^iPr_2C_6H_3)]_2(CH)C\}Pb\{N(SiMe_3)\}_2]$ $(Li(THF)_2{\cdot}$***4***$)$. To a solution of $[:C[N(2,6\text{-}^iPr_2C_6H_3)]_2(CH)CLi]_\infty$ (286 mg, 0.726 mmol) in THF (10 mL) was added and solution of $Pb[N(SiMe_3)_2]_2$ (192 mg, 0.363 mmol) in THF (5 mL) with stirring at ambient temperature.

The dark orange solution was allowed to stir for 30 minutes before being concentrated to 5 mL. With vigorous stirring, hexane (25 mL) was added to induce precipitation of the product as a pale orange crystalline powder. The solution was filtered and the solid washed again with hexane (10 mL) before being dried thoroughly under vacuum (321 mg, 68% yield). Single crystals suitable for single crystal X-ray diffraction were grown by layering a THF solution with hexane. Anal. Calcd for $C_{68}H_{104}LiN_5O_2PbSi_2$ (1293.92): C 63.12%, H 8.10%, N 5.41%. Found: C 62.90%, H 7.98%, N 5.48%. ^{1}H NMR (500.30 MHz, d_8-THF): δ (ppm) 7.10–7.27 (m, 12H; *meta*-Dipp and *para*-Dipp); 6.99 (s, 2H; NCC*H*N); 3.62 (m, 8H; THF); 2.98 (sept, $^3J_{H–H}$ = 7 Hz, 2H; $C_6H_3\{CH(CH_3)_2\}_2$); 2.91 (sept, $^3J_{H–H}$ = 7 Hz, 2H; $C_6H_3\{CH(CH_3)_2\}_2$); 2.90 (sept, $^3J_{H–H}$ = 7 Hz, 2H; $C_6H_3\{CH(CH_3)_2\}_2$); 2.83 (sept, $^3J_{H–H}$ = 7 Hz, 2H; $C_6H_3\{CH(CH_3)_2\}_2$); 1.77 (m, 8H; THF); 1.28 (d, $^3J_{H–H}$ = 7 Hz, 3H; $C_6H_3\{CH(CH_3)_2\}_2$); 1.14 (d, $^3J_{H–H}$ = 7 Hz, 3H; $C_6H_3\{CH(CH_3)_2\}_2$); 1.12 (d, $^3J_{H–H}$ = 7 Hz, 3H; $C_6H_3\{CH(CH_3)_2\}_2$); 1.10 (d, $^3J_{H–H}$ = 7 Hz, 3H; $C_6H_3\{CH(CH_3)_2\}_2$); 1.08 (d, $^3J_{H–H}$ = 7 Hz, 3H; $C_6H_3\{CH(CH_3)_2\}_2$); 1.03 (d, $^3J_{H–H}$ = 7 Hz, 3H; $C_6H_3\{CH(CH_3)_2\}_2$); 1.00 (d, $^3J_{H–H}$ = 7 Hz, 3H; $C_6H_3\{CH(CH_3)_2\}_2$); 1.86 (d, $^3J_{H–H}$ = 7 Hz, 3H; $C_6H_3\{CH(CH_3)_2\}_2$); –0.22 (s, 18H; $N(Si(CH_3)_3)_2$). ^{13}C{^{1}H} NMR (125.80 MHz, d_8-THF): δ (ppm) 210.1 (v br, fwhm = 90 Hz; CN_2); 192.3 (NCCHN); 147.7, 147.6, 147.0 146.7 (*ortho*-Dipp); 143.4, 141.1 (*ipso*-Dipp); 134.7 (NCCHN); 128.4, 128.1 (*para*-Dipp); 124.0, 123.9, 123.5, 123.2 (*meta*-Dipp); 68.4 (THF); 29.2, 28.9, 28.8, 28.7 ($C_6H_3\{CH(CH_3)_2\}_2$); 26.6 (THF); 26.3, 26.2, 25.32, 25.29, 25.2, 25.1, 24.4, 23.1 ($C_6H_3\{CH(CH_3)_2\}_2$); 7.4 ($N(Si(CH_3)_3)_2$). ^{207}Pb{^{1}H} NMR (104.59 MHz, d_8-THF): δ (ppm) 1619.2 (s).

5. Acknowledgements

We thank the EPSRC, the University of Oxford and Christ Church College for financial support of this research (DTA studentship J.B.W.). We also thank the University of Oxford

for access to Chemical Crystallography facilities and Elemental Microanalysis (Devon) for performing the elemental analyses. Special acknowledgement is also given to Dr. Nick Rees for his help with NMR studies.

6. Conflict of interests.

The authors declare no competing financial interests.

Electronic Supplementary Information. CCDC 1548303−1548306 contain the supplementary crystallographic data for this paper (https://www.ccdc.cam.ac.uk/structures/). NMR spectra and computational details are also available.

7. References

[1] Ingleson, M. J.; Layfield, R. A. *Chem. Commun.* **2012**, *48*, 3579–3589; (b) Cazin, C. S. *N-Heterocyclic Carbenes in Transition Metal Catalysis and Organocatalysis*; Springer: Netherlands, 2011; (c) Mercs, L.; Albrecht, M. *Chem. Soc. Rev.* **2010**, *39*, 1903–1912. (d) Díez-González, S. *N-Heterocyclic Carbenes: From Laboratory Curiosities to Effective Synthetic Tools*; RSC Publishing: Cambridge, 2010. (e) Bourissou, D.; Guerret, O.; Gabbaï, F. P.; Bertrand, G.; *Chem. Rev.* **2009**, *100*, 39–91. (f) Jacobsen, H.; Correa, A.; Poater, A.; Costabile, C.; Cavallo, L. *Coord. Chem. Rev.* **2009**, *253*, 687–703. (g) Díez-González, S.; Marion, N.; Nolan, S. P. *Chem. Rev.* **2009**, *109*, 3612–3676. (h) Hahn, F. E.; Jahnke, M. C. *Angew. Chem. Int. Ed.* **2008**, *47*, 3122–3172. (i) Díez-González, S.; Nolan, S. P. *Coord. Chem. Rev.* **2007**, *251*, 874–883. (j) Glorius F. *N-Heterocyclic Carbenes in Transition Metal Catalysis (Topics in Organometallic Chemistry 21)*; Springer-Verlag: Berlin-Heidelberg, Germany, 2006. (k) Nolan S. P. *N-Heterocyclic Carbenes in Synthesis*; Wiley-VCH: Weinheim, Germany, 2006; (l) Bertrand G. *Carbene Chemistry: From Fleeting Intermediates*

to Powerful Reagents; Marcel Dekker: New York, 2002; (m) Herrmann, W. A. *Angew. Chem. Int. Ed.* **2002**, *41*, 1290–1309.

[2] (a) Wang, Y.; Robinson, G. H. *Inorg. Chem.* **2014**, *53*, 11815–11832; (b) Braunschweig, H.; Dewhurst, R. D. *Organometallics* **2014**, *33*, 6271–6277; (c) Rivard, E. *Dalton Trans.* **2014**, *43*, 8577–8586; (d) Frenking, G.; Tonner, R. *The Chemical Bond: Chemical Bonding Across the Periodic Table*; Wiley-VCH: Weinheim, Germany, 2014, pp. 71–112; (e) Ghadwal, R. S.; Azhakar, R.; Roesky, H. W. *Acc. Chem. Res.* **2013**, *46*, 444–456 (f) Wang, Y.; Robinson, G. H. *Dalton Trans.* **2012**, *41*, 337–345.

[3] Arduengo III, A. J.; Harlow, R. L.; Kline, M. *J. Am. Chem. Soc.* **1991**, *113*, 361–363.

[4] Wang, Y.; Xie, Y.; Abraham, W. Y.; Wei, P.; Schaefer, H. F.; Schleyer, P. v. R.; Robinson, G. H. *J. Am. Chem. Soc.* **2010**, *132*, 14370–14372.

[5] For recent reviews see: (a) Waters, J. B.; Goicoechea, J. M. *Coord. Chem. Rev.* **2015**, *293–294*, 80–94; (b) Ghadwal, R. S. *Dalton Trans.* **2016**, *45*, 16081–16095; (c) Nasr, A.; Winkler, A.; Tamm, M. *Coord. Chem. Rev.* **2016**, *316*, 68–124.

[6] (a) Waters, J. B.; Goicoechea, J. M. *Dalton Trans.* **2014**, *43*, 14239–14248; (b) El-Hellani, A.; Lavallo, V. *Angew. Chem. Int. Ed.* **2014**, *53*, 4489–4493; (c) Martínez-Martínez, A. J.; Fuentes, M. A.; Hernán-Gómez, A.; Hevia, E.; Kennedy, A. R.; Mulvey, R. E.; O'Hara, C. T. *Angew. Chem. Int. Ed.* **2015**, *54*, 14075 –14079.

[7] (a) Ellul, C. E.; Mahon, M. F.; Saker, O.; Whittlesey, M. K. *Angew. Chem. Int. Ed.* **2007**, *46*, 6343–6345; (b) Crittall, M. R.; Ellul, C. E.; Mahon, M. F.; Saker, O.; Whittlesey, M. K. *Dalton Trans.* **2008**, 4209–4211; (c) Scheele, U. J.; Dechert, S.; Meyer, F. *Chem. Eur. J.* **2008**, *14*, 5112–5115; (d) Krüger, A.; Kluser, E.; Müller-Bunz, H.; Neels, A.; Albrecht, M. *Eur. J. Inorg. Chem.* **2012**, 1394–1402; (e) Arnold, P. L.; Liddle, S. T. *Organometallics* **2006**, *25*, 1485–1491; (f) Arnold, P. L.; Rodden, M.; Wilson, C.; *Chem. Commun.* **2005**, 1743–1745; (g) Musgrave, R. A.; Turbervill, R. S. P.; Irwin, M.; Goicoechea, J. M. *Angew.*

Chem. Int. Ed. **2012**, *51*, 10832–10835; (h) Waters, J. B.; Turbervill, R. S. P.; Goicoechea, J. M. *Organometallics* **2013**, *32*, 5190–5200; (i) Musgrave, R. A.; Turbervill, R. S. P.; Irwin, M.; Herchel, R.; Goicoechea, J. M. *Dalton Trans.* **2014**, *43*, 4335–4344; (j) Wang, Y.; Xie, Y.; Abraham, M. Y.; Gilliard Jr., R. J.; Wei, P.; Campana, C. F.; Schaefer III, H. F.; Schleyer, P. v. R.; Robinson, G. H. *Angew. Chem. Int. Ed.* **2012**, *51*, 10173–10176; (k) Armstrong, D. R.; Baillie, S. E.; Blair, V. L.; Chabloz, N. G.; Diez, J.; Garcia-Alvarez, J.; Kennedy, A. R.; Robertson, S. D.; Hevia, E. *Chem. Sci.* **2013**, *4*, 4259–4266; (l) Pranckevicius, C.; Stephan, D. W. *Chem. Eur. J.* **2014**, *20*, 6597–6602; (m) Zlatogorsky, S.; Ingleson, M. J. *Dalton Trans.* **2012**, *41*, 2685–2693; (n) Maddock, L. C. H.; Cadenbach, Y.; Kennedy, A. R.; Borilovic, I.; Aromí, G.; Hevia, E. *Inorg. Chem.* **2015**, *54*, 9201−9210; (o) Simler, T.; Braunstein, R.; Danopoulos, A. A. *Chem. Commun.* **2016**, *52*, 2717−2720; (p) Schwedtmann, K.; Schoemaker, R.; Hennersdorf, F.; Bauzá, A.; Frontera, A.; Weiss, R.; Weigand, J. J. *Dalton Trans.* **2016**, *45*, 11384–11396; (q) Winkler, A.; Brandhorst, K.; Freytag, M.; Jones, P. G.; Tamm, M. *Organometallics* **2016**, *35*, 1160−1169; (r) Bitzer, M. J.; Kühn, F. E.; Baratta, W. *J. Catal.* **2016**, *338*, 222–226; (s) Valyaev, D. A.; Uvarova, M. A.; Grineva, A. A.; César, V.; Nefedov, S. N.; Lugan, N. *Dalton Trans.* **2016**, *45*, 11953–11957; (t) Specklin, D.; Fliedel, C.; Gourlaouen, C.; Bruyere, J.-C.; Avil, T.; Boudon, C.; Ruhlmann, L.; Dagorne, S. *Chem. Eur. J.* **2017**, *23*, 5509–5519.

[8] (a) Wang, Y.; Xie, Y.; Abraham, M. Y.; Gilliard Jr., R. J.; Wei, P.; Schaefer III, H. F.; Schleyer, P. v. R.; Robinson, G. H. *Organometallics* **2010**, *29*, 4778–4780; (b) Jana, A.; Azhakar, R.; Tavčar, G.; Roesky, H. W.; Objartel, I.; Stalke, D.; *Eur. J. Inorg. Chem.* **2011**, 3686–3689; (c) Wang, Y.; Xie, Y.; Abraham, M. Y.; Wei, P.; Schaefer III, H. F.; Schleyer, P. v. R.; Robinson, G. H. *Organometallics* **2011**, *30*, 1303–1306; (d) Wang, Y.; Abraham, M. Y.; Gilliard Jr., R. J.; Wei, P.; Smith, J. C.; Robinson, G. H. *Organometallics*, **2012**, *31*, 791–793; (e) Chen, M.; Wang, Y.; Gilliard, Jr., R. J.; Wei, P.; Schwartz, N. A.; Robinson, G. H.

Dalton Trans. **2014**, *43*, 14211–14214; (f) Kronig, S.; Theuergarten, E.; Daniliuc, C. G.; Jones, P. G.; Tamm, M. *Angew. Chem. Int. Ed.* **2012**, *51*, 3240–3244; (g) Ghadwal, R. S.; Reichmann, S. O.; Carl, E.; Herbst-Irmer, R. *Dalton Trans.* **2014**, *43*, 13704–13710; (h) Uzelac, M.; Hernán-Gómez, A.; Armstrong, D. R.; Kennedy, A. R.; Hevia, E. *Chem. Sci.* **2015**, *6*, 5719–5728; (i) Wang, Y.; Xie, Y.; Wei, P.; Schaefer III, H. F.; Robinson, G. H. *Dalton Trans.* **2016**, *45*, 5941–5944; (j) Kumar, P.; Keith, M.; Chow, C. F.; Hsieh, T. H. H.; Bowes, E. G.; Schnakenburg, G.; Kennepohl, P.; Streubel, R.; Gates, D. P. *Chem. Commun.* **2016**, *52*, 998–1001; (k) Winkler, A.; Freytag, M.; Jones, P. G.; Tamm, M. *Z. Anorg. Allg. Chem.* **2016**, *642*, 1295–1303; (l) Uzelac, M.; Kennedy, A. R.; Hernán-Gómez, A.; Fuentes, M. A.; Hevia, E. *Z. Anorg. Allg. Chem.* **2016**, *642*, 1241–1244.

[9] Eymann, L. Y. M.; Scopelliti, R.; Fadaei, F. T.; Cecot, G.; Solari, E.; Severin, K. *Chem. Commun.* **2017**, *53*, 4331–4334.

[10] Bradley, D. C.; Dawes, H. M.; Hursthouse, M. B.; Powell, H. R. *Polyhedron* **1988**, *7*, 2049–2051.

[11] Yu, X.; Bi, S.; Guzei, I. A.; Lin, Z.; Xue, Z.-L. *Inorg. Chem.* **2004**, *43*, 7111–7119.

[12] Veith, M.; Gasthauer, M.; Zimmer, M.; Huch, V. *Z. Anorg. Allg. Chem.* **2007**, *633*, 2274–2277.

[13] Bell, N. L.; Maron, L.; Arnold, P. L. *J. Am. Chem. Soc.* **2015**, *137*, 10492–10495.

[14] Johnson, K. R. D.; Hayes, P. G. *Polyhedron* **2016**, *108*, 43–49.

[15] Chalk, A. J.; Hoogeboom, T. J. *J. Organomet. Chem.* **1968**, *11*, 615–618.

[16] Mitchell, T. N. *J. Organomet. Chem.* **1974**, *70*, C1–C2.

[17] Yang, L.; Powell, D. R.; Houser, R. P. *Dalton Trans.* **2007**, 955–964.

[18] Okuniewski, A.; Rosiak, D.; Chojnacki, J.; Becker, B. *Polyhedron* **2015**, *90*, 47–57.

[19] (a) Wagner, M.; Zöller, T.; Hiller, W.; Prosenc, M. H.; Jurkschat, K. *Chem. Commun.* **2013**, *49*, 8925–8927; (b) Singh, A. P.; Samuel, P. P.; Mondal, K. C.; Roesky, H. W.; Sidhu,

N. S.; Dittrich, B.; *Organometallics* **2013**, *32*, 354–357; (c) Turbervill, R. S. P; Goicoechea, J. M. *Aust. J. Chem.* **2013**, *66*, 1131–1137.

[20] Pyykkö, P.; Atsumi, M. *Chem. Eur. J.* **2009**, *15*, 186–197.

[21] Cordero, B.; Gómez, V.; Platero-Prats, A. E.; Revés, M.; Echeverría, J.; Cremades, E.; Barragán, F.; Alvarez, S. *Dalton Trans.* **2008**, 2832–2838.

[22] Preut, H.; Haupt, H.-J.; Huber, F. *Z. Anorg. Allg. Chem.* **1973**, *396*, 81–89.

[23] Flack, H. D.; Bernardinelli, G. *Chirality* **2008**, *20*, 681–690.

[24] Bürger, H.; Sawodny, W.; Wannagat, U. *J. Organomet. Chem.* **1965**, *3*, 113–120.

[25] Gynane, M. J. S.; Harris, D. M.; Lappert, M. F.; Power, P. P.; Rivière, P.; Rivière-Baudet, M. *J. Chem. Soc., Dalton Trans.* **1977**, 2004–2009.

[26] Cosier, J.; Glazer, A. M. *J. Appl. Crystallogr.* **1986**, 105–107.

[27] Otwinowski, Z.; Minor, W. *Macromol. Crystallogr. Part A* **1997**, *276*, 307–326.

[28] Palatinus, L.; Chapius, G. J. Appl. Crystallogr., 2007, 40, 786–790.

[29] (a) Sheldrick, G. M. SHELXL97, Programs for Crystal Structure Analysis (Release 97-2) 1998; (b) Sheldrick, G. M. *Acta Crystallogr. Sect. A.* **1990**, *46*, 467–473; (c) Sheldrick, G. M. *Acta Crystallogr. Sect. A.* **2008**, *64*, 112–122.

TOC graphic

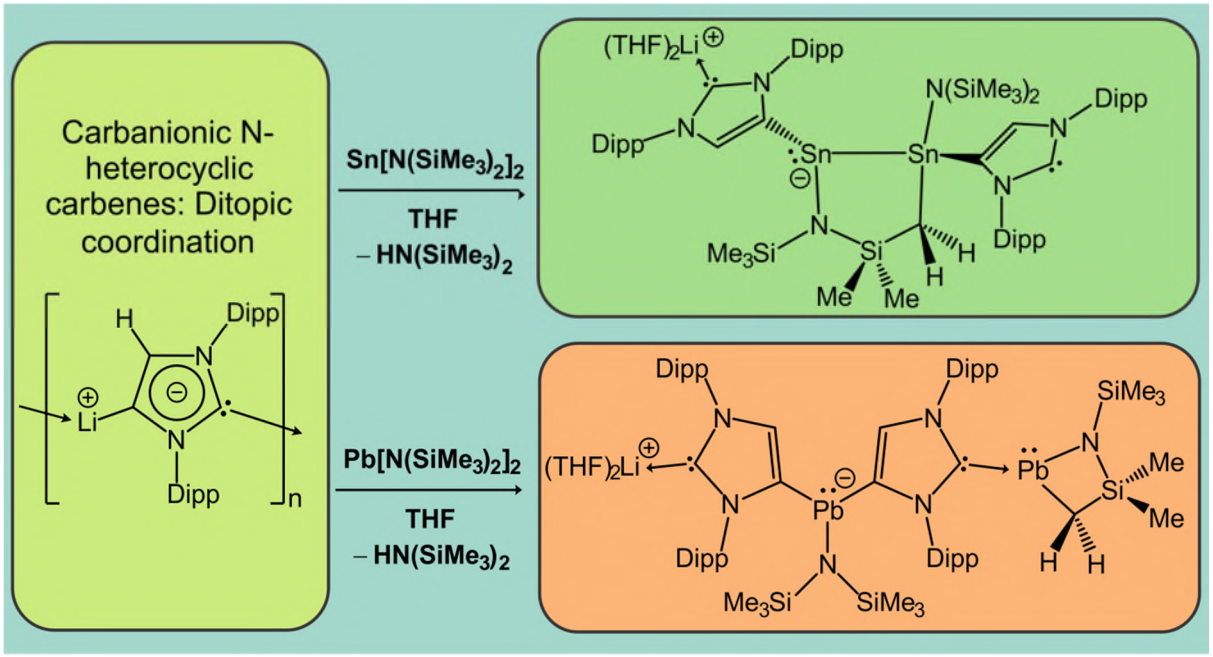
Carbanionic N-heterocyclic carbenes: Ditopic coordination
Sn[N(SiMe3)2]2
THF
– HN(SiMe3)2
Pb[N(SiMe3)2]2
THF
– HN(SiMe3)2
(THF)2Li
Dipp
N(SiMe3)2
Me3Si
SiMe3
Me
H
Pb
Sn
Si
N
Li
n